

Accepted Manuscript

The role of weak interactions in self-assembly of supramolecular associations of benzothiazole derivatives and their coordination compounds

Alma Lilia García-Ortiz, Ricardo Domínguez-González, Margarita Romero-Ávila, Blas Flores-Pérez, Luis Guillén, Miguel Castro, Norah Barba-Behrens

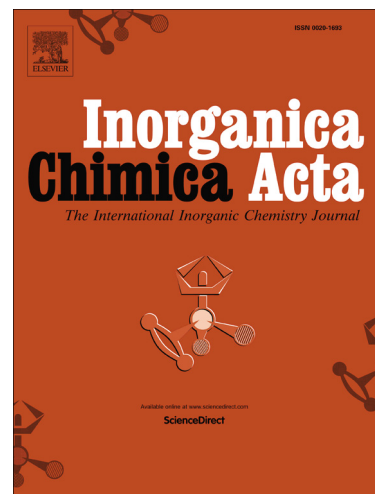
PII: S0020-1693(17)31267-7
DOI: <https://doi.org/10.1016/j.ica.2017.10.012>
Reference: ICA 17939

To appear in: *Inorganica Chimica Acta*

Received Date: 9 August 2017
Revised Date: 4 October 2017
Accepted Date: 11 October 2017

Please cite this article as: A.L. García-Ortiz, R. Domínguez-González, M. Romero-Ávila, B. Flores-Pérez, L. Guillén, M. Castro, N. Barba-Behrens, The role of weak interactions in self-assembly of supramolecular associations of benzothiazole derivatives and their coordination compounds, *Inorganica Chimica Acta* (2017), doi: <https://doi.org/10.1016/j.ica.2017.10.012>

This is a PDF file of an unedited manuscript that has been accepted for publication. As a service to our customers we are providing this early version of the manuscript. The manuscript will undergo copyediting, typesetting, and review of the resulting proof before it is published in its final form. Please note that during the production process errors may be discovered which could affect the content, and all legal disclaimers that apply to the journal pertain.



The role of weak interactions in self-assembly of supramolecular associations of benzothiazole derivatives and their coordination compounds

Alma Lilia García-Ortiz^a, Ricardo Domínguez-González^a, Margarita Romero-Ávila^b, Blas Flores-Pérez^b, Luis Guillén^c, Miguel Castro^c, Norah Barba-Behrens^{a*}

^aDepartamento de Química Inorgánica, Facultad de Química, Universidad Nacional Autónoma de México, Ciudad Universitaria, Coyoacán, Ciudad de México. 04510, México

^bDepartamento de Química Orgánica, Facultad de Química, Universidad Nacional Autónoma de México, C. U., Coyoacán, Ciudad de México. 04510, México

^cDepartamento de Física y Química Teórica, Facultad de Química, Universidad Nacional Autónoma de México, C. U., Coyoacán, Ciudad de México. 04510, México

Corresponding author

E-mail address: norah@unam.mx (N. Barba-Behrens)

Tel/fax: 52(55)5622-3810

Abstract

New benzothiazole derivatives and their transition metal coordination compounds were synthesized and structurally characterized. The participation of weak interactions, as H-bonding, π -stacking, O \rightarrow S, N \rightarrow S and S lone pair $\cdots\pi$, on the stabilization of their supramolecular assemble was analyzed.

The bis-benzothiazole (ebbtz) derivative was obtained from the reaction of benzothiazole-2-carboxaldehyde and ethylenediamine. When reacting this ligand with copper(II) chloride, an electrophilic addition of methanol, as a methoxy group, gave place to the amino ether derivative on the coordination compound [Cu(MeO-ebbtz)Cl]Cl \cdot 4H₂O. The supramolecular arrangement of this compound is stabilized by H-bonding, O \rightarrow S, N \rightarrow S, lp(S) $\cdots\pi$ and π -stacking interactions. Whereas, from the reaction *in situ* of benzothiazole-2-carboxaldehyde, ethylenediamine and copper(II) bromide, the polymeric [Cu₂(μ -Br)₃(ebtz)Br]_n compound was obtained. In this compound, the copper(II) atoms present two different geometries, tetrahedral and octahedral, where a 3D assembly is driven by lp(S) $\cdots\pi$ and $\pi\cdots\pi$ stacking.

Two isostructural [M(H₂O)₂(CH₃OH)₄] \cdot 2(prbtz) (M = Co^{II} and Ni^{II}) compounds and a polymeric sodium complex were obtained with 3-(benzothiazol-2-ylthio)-1-propanesulfonate (prbtz). In the [Na₂(prbtz)₂(H₂O)₂ μ -(H₂O)]_n polymer, the prbtz⁻ is bound to the metal ion in a bent conformation, presenting a supramolecular arrangement stabilized by H-bonding, N \rightarrow S, T-shape and lp(S) $\cdots\pi$ interactions. On the other hand, in the [M(H₂O)₂(CH₃OH)₄] \cdot 2(prbtz) compounds, prbtz⁻ co-crystallized, presenting an extended conformation, mainly with lp(S) $\cdots\pi$ interactions.

Additionally, theoretical calculations on the association between two ebbtz molecules, were performed. The results indicate that these molecules have a binding energy of 79.49 kJ/mol promoted by lp(S) $\cdots\pi$ and $\pi\cdots\pi$ stacking interactions, taking place at the frontier LUMO and HOMO molecular orbitals.

Keywords: benzothiazole derivatives; transition metal compounds; lp(S) $\cdots\pi$; $\pi\cdots\pi$ stacking, N \rightarrow S and O \rightarrow S interactions; supramolecular arrangements

Introduction

Weak interactions have been studied for some time, where the most analyzed is the classical hydrogen bonding ($D-H\cdots A$), formed between polar species $D-H$ and a lone pair carrier A (electron rich atom). They are characterized for a weak to medium interaction energy (ca. 10-40 kJ/mol), a substantial overlap of electron density of the heteroatoms, electron transfer between the heteroatoms and with preferred bond lengths from 2.2 Å to 3.2 Å ($D\cdots A$), and angles from 90° to 180° ($D-H\cdots A$) [1–3].

Interactions between aromatic rings have also been widely studied since 1985 when Burley and Petsko proved their importance in their pioneering work on DNA and proteins. It was stated that there is a competition between stacking and T-shape arrangements on interacting aromatic rings, with very low energy difference (0-50 kJ/mol) [4,5].

Recently, it has been an increasing interest on sulfur-containing molecules, where the sulfur atom may behave as a Lewis base or Lewis acid, due to its capability to act as an electron donor as consequence of the directionality of their lone pairs, or as an electron acceptor driven by a hypervalent behavior towards a pseudo trigonal bipyramidal geometry.[6–8] The latter could be defined as weak donor-acceptor interactions, $Y\rightarrow S$; where Y is a main group element, an electron rich atom with lone-pair (lp) electrons in the n_o direction, N or O, that interacts with a $S \sigma^*$ orbital of a positive potential [9,10]. Both, the $Y\rightarrow S$ interaction and the $S \sigma^*$ orbital are oriented in the same plane, different from the out of the plane interaction in the π_o direction, which is observed for a carbonyl group[11]. These type of intermolecular associations have been found for molecules containing $P\rightarrow S$, $Cl\rightarrow S$, $Sn\rightarrow S$ and $Si\rightarrow S$ interactions [12,13].

The $S\rightarrow S$ interaction has been considered as a “weak contact”, taking into account that the distance between them is not larger than 3.7 Å (Σ Van der Waals radii) [7], while, for $O\rightarrow S$ and $N\rightarrow S$ are 3.32 and 3.35 Å, respectively [11].

Hypervalent $Y\rightarrow S$ interactions may control the molecular structure and the formation of different patterns of association as shape, size and packing, in addition to the chemical reactivity of organic molecules and coordination compounds [14–19]. Lone pair $\cdots\pi$ short contacts ($lp\cdots\pi$), have been less studied. Nevertheless, computational studies have demonstrated that such interactions, between a lp donor and an aromatic ring acceptor can be energetically favorable, the

maximum distance, from the lp donor to the aromatic ring centroid being of 3.82 Å [20–22]. However, in the case of S $\cdots\pi$ interactions, distances in the range of 3.5–4.9 Å [4]. An example of this type of interaction is shown in the X-ray crystal structure of the lysozyme protein (PDB 6LYZ), figure SI 1, where the distances lp(S) $\cdots\pi$ to the centroids of five membered rings are in the range of 3.9–4.4 Å. These weak interactions are relevant for some organic molecules, stabilizing a thermo-dependent conformation and restricting its rotation [23].

All these contributions are also important for maintaining folded protein structures and their thermal stability [8]. Many of these interactions have been found on proteins by X-ray diffraction analysis from databases and computational studies [24–26].

On the other hand, in the biological activity of some sulfur containing molecules, the conformation stabilized by intra and inter molecular interactions Y \rightarrow S, plays a crucial role, in antiangiogenic drugs [27,28] or in the treatment of inflammatory diseases, such as rheumatoid arthritis [29]. The understanding of these interactions will contribute to elucidate their mechanism of action [30] and into the development of new drugs [26,31], for example, the treatment of Chagas' disease [32–34].

In this context, we studied different benzothiazole derivatives and their transition metal coordination compounds. The role of weak interactions, as Y \rightarrow S (Y = N, O), lp(S) $\cdots\pi$, $\pi\cdots\pi$ H $\cdots\pi$ (T-shape) and hydrogen bonding, on the stabilization of 3D crystal assembling was analyzed.

2. Experimental

2.1 General

The sodium 3-(benzothiazol-2-ylthio)-1-propanesulfonate (Aldrich), metal salts (Baker) and solvents (THF and acetone, Baker; anhydrous MeOH, Aldrich) were commercial and used without further purification. FT IR spectra in the range 4000–400 cm⁻¹ were collected in a Perkin Elmer FT-IR Spectrum 400 spectrophotometer with a universal ATR sampling, accessory at 298 K. Electronic spectra were measured over the range 40,000–5000 cm⁻¹ by the diffuse reflectance method on a Cary-5000 Varian spectrophotometer at 298 K. Mass spectra (MS-ESI+) were determined in a Thermo Trace GC Ultra (capilar colum DB5) mass spectrometer. Elemental (C,

N, H, S) analyses were made on a Perkin Elmer 2400 analyzer. $^1\text{H-NMR}$ and $^{13}\text{C-NMR}$ spectra were recorded on a Varian 400 MHz instrument using TMS as internal reference in CDCl_3 .

2.2 X-ray crystallographic study

Diffraction data were collected on a Bruker Smart APEX II or on a Xcalibur, Atlas, Gemini diffractometer with a CCD area detector and Mo K_α radiation source ($\lambda = 0.71073 \text{ \AA}$). APEX2 or CrysAlisPro software packages were used for data collection and data integration. The compounds were collected at RT (130 K) and the structures were solved by Direct Methods using SHELXT 2014/5 (Sheldrick, 2014) and refined by full-matrix least-squares on F^2 with SHELXL-2016/6 (Sheldrick, 2016) [35] using the ShelXle GUI. Anisotropic displacement parameters were used for all non-H atoms. Hydrogen atoms for the C-H bonds were placed in idealized positions and refined using a riding model. The H atoms attached to O or N atoms were found in difference Fourier map and their position were refined with U_{iso} parameter equal to 1.2 times the equivalent parameter of the atom to which they are attached with distance restraints (DFIX). The disordered groups and solvent were refined using geometry (SAME, SADI) and U_{ij} restraints (SIMU, RIGU) by SHELXL. Molecular graphics were preparing using Mercury, POV-RAY and PAINT.NET programs. Crystallographic data are listed in Table 1 and Table 2.

Table 1.

Table 2.

2.3 Synthesis of the compounds

2.3.1 Synthesis of benzothiazole-2-carboxaldehyde (*btzca*)

Benzothiazole-2-carboxaldehyde was synthesized using a previously reported procedure [36] from benzothiazole by eliminating of the proton in the position 2 with *n*-BuLi, followed by a neutralization. A solution of *n*BuLi in hexane (2mL, 2M) was slowly added to a solution of benzothiazole (0.5023g, 3.7mmol) in dry THF (5mL) at -78 °C. Then a solution DMF in THF (18.5mmol, 1.4mL) was dropped into the mixture and finally neutralized. A yellow powder was obtained. The product was purified by a chromatography column with an AcOEt-hexane solution (1:50). Needle crystals were obtained by re-crystallization with dichloromethane. After the purification, this precursor was characterized by ¹H-NMR (400 MHz, CDCl₃): δ 10.17 (s, 1H), 8.25 (ddd J=9.5, 6.6, 5.2, 0.7 Hz, 1H), 8.00 (ddd, J=9.4, 6.3, 5.0, 0.7 Hz, 1H), 7.59 (dq, J=7.9, 7.2, 1.5 Hz, 2H), 7.57 (s, 1H) and 7.62 (s, 1H) Fig. SI 2. ¹³C-NMR (400 MHz, CDCl₃): δ = 185, 165, 153, 136, 122, 125, 127 and 128. Fig. SI 3 MS(ESI): *m/z* = 163.

2.3.2 *Ebbtz* ligand

This ligand was obtained from benzothiazole-2-carboxaldehyde (1.1557g, 7.08mmol) and ethylenediamine (3.54mmol) in methanol (40mL) at 20h reflux. The colorless needles crystals were characterized by M.P. 184-185°C. Mol. Wt: 350.46g/mol. Anal. Calc. for C₁₈H₁₄N₄S₂: C, 61.68; H, 4.02; N, 15.98; S, 18.29%. Found: C, 61.89; H, 3.39; N, 16.37; S, 17.81%. MS(ESI): *m/z* = 350 [M + H⁺]. FT-IR (ATR, cm⁻¹) ν(C=N) aliphatic 1636; ν(C=N) ring 1498-1455; ν_s(C=C) 1590, ν_{as}(C=C) 1316. ¹H-NMR (400 MHz, CDCl₃): δ 8.65 (s, 1H), 4.09 (s, 2H), 8.11 (ddd, J= 9.3, 6.4, 5.3, 0.6 Hz, 1H), 8.05 (ddd, J=9.4, 6.7, 5.5, 0.7 Hz, 1H), 7.52 (tt, J=8.2, 7.6, 7.2, 2.0 Hz, 2H). Fig. SI 4 ¹³C-NMR (400 MHz, CDCl₃): δ = 60, 123, 127, 134, 153, 158 and 167. Fig. SI 5.

2.3.3 [Cu(MeO-*ebbtz*)Cl]Cl·4H₂O

An anhydrous methanol solution of CuCl₂·6H₂O (17.1 mg, 0.1 mmol) was added to a 10mL anhydrous methanol solution of *ebbtz* (0.0348 g, 0.1 mmol). The reaction mixture was heated under reflux with constant stirring during 3 h. The obtained blue solution was let to stand at RT, after 15 days, blue crystals were formed which were collected and analyzed by X-ray diffraction.

FT-IR (ATR, cm^{-1}): $\nu(\text{C}=\text{N})_{\text{alip}}$. 1598, $\nu(\text{C}=\text{N})_{\text{ring}}$ 1474, $\nu(\text{C}-\text{O})$ 1057. UV-Vis-NIR ν (cm^{-1}): $\nu_1 = 14133$.

2.3.4 $[\text{Cu}_2(\mu\text{-Br})_3(\text{ebtz})\text{Br}]_n$

A solution of $\text{CuBr}_2 \cdot 6\text{H}_2\text{O}$ (223.35 mg, 1 mmol) in THF was added to a benzothiazole-2-carboxaldehyde solution (81.5 mg, 0.5 mmol) in THF (10 mL), stirred for 30 minutes then ethylenediamine (0.5 mmol) was added in order to obtain the Schiff base *in situ*. The obtained green solution was left to stand at RT, after 30 days, green lamina crystals were formed. UV-Vis-NIR ν (cm^{-1}): $\nu_1 = 14500$.

2.3.5 $[\text{Cu}(\text{ebtz})\text{Br}]\text{Br} \cdot \text{H}_2\text{O}$

The same procedure as for 2.3.4, was followed to obtain this compound, changing the solvent for acetone. The obtained green solution was left to stand at RT, after 30 days, green prism crystals were formed, but the X-ray crystal diffraction data were not good enough, but connectivity between the atoms was adequate for the molecular structure. UV-Vis-NIR ν (cm^{-1}): $\nu_1 = 13776$.

2.3.6 $[\text{Co}(\text{CH}_3\text{OH})_4(\text{H}_2\text{O})_2] \cdot 2(\text{prbtz})$

An aqueous solution, 20 mL, of Naprbtz (312 mg, 1.02 mmol) was mixed with $\text{Co}(\text{NO}_3)_2 \cdot 6\text{H}_2\text{O}$ (611 mg, 2.10 mmol), and left under reflux for 24 h. After this time, the reaction was evaporated and the precipitate was filtered, which corresponds to the $\text{Na}[\text{Co}(\text{prbtz})_2(\text{NO}_3)(\text{H}_2\text{O})] \cdot 6\text{H}_2\text{O}$ compound, which was washed with cool EtOH. Anal. Calcd. C, 28.84; H, 4.30; N, 4.73; S, 21.39. Found C, 28.37; H, 4.05; N, 4.97; S, 22.60%.

The $\text{Na}[\text{Co}(\text{prbtz})_2(\text{NO}_3)(\text{H}_2\text{O})] \cdot 6\text{H}_2\text{O}$ compound (100 mg) was dissolved in methanol (5 mL) and left to stand at RT. After one week pale pink crystals of the $[\text{Co}(\text{CH}_3\text{OH})_4(\text{H}_2\text{O})_2] \cdot 2(\text{prbtz})$ compound, were obtained which were suitable for X-ray diffraction analysis.

2.3.7 $[\text{Ni}(\text{CH}_3\text{OH})_4(\text{H}_2\text{O})_2] \cdot 2(\text{prbtz})$

An aqueous solution, 20 mL of Naprbtz (308 mg, 1.0 mmol) was mixed with $\text{Ni}(\text{NO}_3)_2 \cdot 6\text{H}_2\text{O}$ (588 mg, 2.02 mmol), and left under reflux for 24 h. After this time, the reaction was evaporated and the precipitate was filtered, which corresponds to the $\text{Na}[\text{Ni}(\text{prbtz})_2(\text{NO}_3)(\text{H}_2\text{O})] \cdot 6\text{H}_2\text{O}$

compound, which was washed with cool EtOH. Anal. Calcd. C, 28.38; H, 4.29; N, 4.92; S, 19.70. Found C, 28.40; H, 4.06; N, 4.97; S 22.70%.

The $\text{Na}[\text{Ni}(\text{prbtz})_2(\text{NO}_3)(\text{H}_2\text{O})]\cdot 6\text{H}_2\text{O}$ compound (100 mg) was dissolved in methanol (5mL) and left to stand at RT. After one week, green crystals of the $[\text{Ni}(\text{CH}_3\text{OH})_4(\text{H}_2\text{O})_2]\cdot 2(\text{prbtz})$ compound were obtained, which were suitable for X-ray diffraction analysis.

2.3.8 $[\text{Na}_2(\text{prbtz})_2(\text{H}_2\text{O})_2\mu-(\text{H}_2\text{O})]_n$

A saturated aqueous solution of this compound was prepared, then let to stand at RT. After one week, colorless crystals were observed. Anal. Calcd. C, 38.57; H, 3.24; N, 4.49; S, 30.89%. Found C, 38.95; H, 3.37; N, 3.95; S, 30.64%.

2.4 Computational Procedure.

First principles density functional theory (DFT) calculations were performed for the analysis of the structural, electronic and energetic properties for DRX data of benzothiazole derivatives and their molecular aggregates. All electron calculations were done at the B3LYP level of theory [37,38], jointly with 6-311+G(d, p) basis sets[39-41]. The quantum chemistry software Gaussian 09 was employed.[42] The total energy for a basic building block, two layers, of the systems was determined as this level of theory. The results allow to analyze the basic binding interactions responsible for the stability of the system. Natural bond order (NBO) population analysis were done for the GSs. Charge distributions were estimated also through the B3LYP/6-311+G(d,p) method. The frontier molecular orbitals, LUMO, HOMO and other orbitals involved in the binding interactions of the system were determined.

3. Results and Discussion

Benzothiazole-2-carboxaldehyde (btzca)

The X-ray diffraction analysis of the benzothiazole-2-carboxaldehyde shows a planar conformation of the molecule that is stabilized by the interaction $\text{O}\rightarrow\text{S}$ (3.065 Å; $\Sigma r_{\text{vdw}} = 3.32$ Å), which also promotes that the C1-C8 bond length to be shorter (1.472 Å) than the expected for a C-

C single bond. Also intermolecular associations are observed, through two weak hydrogen bonds C-H \cdots O1 (2.528 and 2.563Å), as depicted in Fig. 1.

Fig. 1.

The planarity of the benzothiazole-2-carboxaldehyde molecules gives place to organized horizontal layers and the only interaction that stabilizes the 3D structure is the $\pi(\text{C}=\text{O})\cdots\pi(\text{aryl})$ staking between them, Fig 2.

Fig. 2.

The benzothiazole-2-carboxaldehyde (btzca) was used as a precursor to obtain the Schiff base N,N'-bis(1,3-benzothiazole-2-ylmethylene)ethane-1,2-diamine ebbtz ligand.

N,N'-bis(1,3-benzothiazole-2-ylmethylene)ethane-1,2-diamine (ebbtz)

The ebbtz ligand was obtained by a classical condensation reaction, where one water molecule is lost, generating azomethine groups (C=N). Its X-ray crystal structure showed that the benzothiazole fragments are symmetrically bound to the ethylenediamine moiety in the ebbtz ligand, the N2-C9-C10-N3 atoms present a small torsion angle of 28.32°, indicating that the complete molecule is in an extended conformation, Fig 3.

Fig. 3.

This extended conformation presents three different N \rightarrow S interactions: two intramolecular N2 \rightarrow S1 and N3 \rightarrow S2 (3.039 Å, 2.97; $\Sigma r_{\text{vdw}} = 3.85$ Å), from the nitrogen atom of the azomethine group to the sulfur from benzothiazole and an intermolecular N4 \rightarrow S1 (3.225 Å), between neighboring molecules, yielding a zig-zag arrangement, Fig 4. The complete 3D network is shown in Fig. SI 6

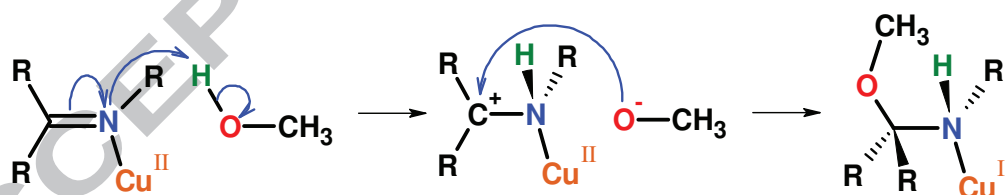
Fig. 4.

Several $\pi\cdots\pi$, $lp(S)\cdots\pi$ and $H\cdots\pi$ intermolecular interactions stabilize the ebbtz crystal network. Two $\pi\cdots\pi$ interactions are observed: face to face, between the benzene and thiazole aromatic ring(S1) from neighboring molecules (3.747 Å) and the azomethine group C11=N3 with the nearest thiazole ring (3.787 Å). The sulfur lone pair $lp(S2)\cdots\pi$ interacts with a benzene ring (3.594 Å), while $lp(S1)$ does this with the azomethine C8=N2 ($S1\cdots\pi$ C8=N2; 3.507 Å). Both methylene groups, present $H\cdots\pi$ interactions, C-H10A $\cdots\pi$ C11=N3 and C-H9B $\cdots\pi$ C8=N2 (2.923Å, 3.076Å) (Fig 5A). Finally, ebbtz blocks are interconnected by $H\cdots\pi$, in a T-shape arrangement (C-H16 $\cdots\pi$, 3.295Å, C-H5 $\cdots\pi$, 3.6.39Å) (Fig5 B).

Fig. 5.



In the synthesis reaction of this compound, the ebbtz ligand presented an aldol condensation by the addition of a methoxy group from the methanol solvent. This reaction was catalyzed by copper(II), where each carbon atom from the azomethine group formed a new ester group through an electrophilic addition, Scheme 1



Scheme 1. Reaction mechanism of the aldolic condensation

The IR spectrum from the ebbtz ligand, shows characteristic bands from the azomethine group (C=N) in the region 1636 cm^{-1} . This band is shifted in the coordination compound to a lower frequency, 1600 cm^{-1} , indicating its coordination through the N atom to the copper(II) center. The $\nu(C=N)$ band of the thiazole ring is at 1500 cm^{-1} in the free ligand, while in the coordination compounds this band is shifted to 1470 cm^{-1} . Upon the addition of the methoxy groups in the

[Cu(MeO-ebbtz)Cl]Cl·4H₂O compound, a new band at 1057 cm⁻¹ was assigned to the $\nu(\text{C-O})$, from the methoxy group.

The X-ray crystal structure of this compound shows a Cu^{II} in a square pyramidal geometry ($\tau=0.03$), where N1 is found in the apical position (length 2.270 Å) and the square base is constituted by N4, N2, N3 (length *ca.* 2.04 Å) and Cl1 (length 2.255 Å), Fig 6.

Fig. 6.

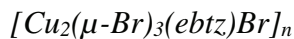
A methoxy group is bound to the C atoms from each azomethine, through an aldol condensation reaction, forming four new chiral centers, C8, C11, N3 and N2.

The [Cu(MeO-ebbtz)Cl]Cl·4H₂O compound shows different hydrogen bonding interactions, promoted by water molecules and the chloride, O4W-H \cdots O3W (2.246 Å), O3W-H \cdots Cl2 (2.361 Å), O2W-H \cdots Cl2 (2.374 Å), O2W-H \cdots Cl2 (2.550 Å), O1W-H \cdots O2W (2.017 Å), N3-H \cdots O1W (2.037 Å), N2-H \cdots Cl2 (2.384 Å), Fig. 7. These associations generate a 3D pleated sheet arrangement, with water channels on the b axis.

Fig. 7.

Intermolecular π stacking, between adjacent heterocycle rings, contribute to the supramolecular structure, Fig. 8. Two neighboring benzene rings are eclipsed with a distance of 3.719 Å and an angle of 95.12°. Additionally, two symmetric parallel contacts, lp(S2) $\cdots\pi$ (3.582 Å) are present. A water molecule gives place to O1W \rightarrow S2, 3.202 Å. Simultaneously intramolecular contributions are also of relevance. A T-shape interaction, C-H2 $\cdots\pi$ from the 6-membered ring with the thiazole ring is observed (3.234 Å). Due to the orientation of the methoxy group it allows two O \rightarrow S intramolecular interactions O2 \rightarrow S2, 2.903 Å and O1 \rightarrow S1, 2.962 Å ($\Sigma r_{vdw} = 3.32$ Å). In Fig. SI 7 is shown the supramolecular arrangement.

Fig. 8.



The DRX analysis (Fig. 9) shows that the asymmetric unit of this polymeric compound contains two copper(II) atoms and the *N*-[(1*H*-benzimidazol-2-yl)methyl]ethane-1,2-diamine (ebt_z) ligand. The Cu₂ atom presents a regular tetrahedral geometry with four coordinated Br atoms, where Br1, Br2 and Br3 participate as a bridge connecting both copper atoms. The observed angles are in the range from 101° to 110°. On the other hand, the Cu1 atom shows a distorted octahedral geometry with a *mer* isomery. Their meridional angles are in the range from 84° to 98° and the axial angles are 161.75° and 169.42°.

Fig. 9.

In this compound, two polymeric chains of $[Cu_2(\mu-Br)_3(ebtz)Br]_n$ are associated by different interactions. One of them is by intercalation of their aromatic rings through weak parallel $lp(S) \cdots \pi(\text{ring})$ (3.571 Å), Fig. 10A, which are in the expected range (3.5-3.82 Å). Additionally, the Br₄ atom participates in a bifurcated hydrogen bonding, C-H \cdots Br₄, with two benzyl ring protons (3.049 and 2.750 Å). This two chains behave as a building block which are interconnected through hydrogen bonding N-H_{3B} \cdots Br₄ (2.75 Å) and C-H₃ \cdots Br₄ (3.150 Å), Fig. 10 B. This 3D arrangement gives place to Br channels on the *c* axis, Fig. SI 8.

Fig. 10.

The X-ray diffraction data of the $[Cu(ebtz)Br]Br \cdot H_2O$ compound was not of the adequate quality to analyze weak interactions. Nevertheless, the connectivity of the copper(II) and the coordinated atoms shows a square base pyramidal geometry, where the square base is formed by a Br and 3 nitrogen atoms, with a water molecule in the apical position. Fig 11.

Fig. 11.

It is interesting that a sulfure lp $\cdots\pi$ (benzene ring) interaction is observed, as well as parallel head to tail associations (Fig 12). The apical coordinated water molecules forms water channels under c axis Fig. SI 9.

Fig. 12.



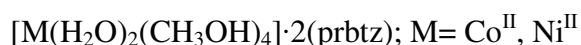
In this coordination compound the asymmetric unit generates a dimer, shown in Fig.13, which is part of a polymeric chain. The dimer is constituted by two sodium atoms in a distorted octahedral geometry with six oxygen atoms, from three water molecules and three from the sulfonate groups. The meridional angles are in the range from 75° to 116° and the axial angles are 160° and 166°. The sodium atoms are interconnected through two O-S-O bridges from the sulfonate groups. One water molecule bridges the sodium metal ions and is found in the cavity formed by an eight-membered ring.

Fig. 13.

On the *c* axis of the extended polymer, N \rightarrow S interactions are found between neighboring ligand molecules (3.296Å) Fig. 14A, as well as bifurcated hydrogen bonds, O4-H \cdots O2 (1.916 Å) and O4-H \cdots O1 (1.996 Å). These chains interact by face to edge contacts C5-H5 $\cdots\pi$ (ring) and lp(S) $\cdots\pi$ (ring) 3.661Å, Fig. 14B, promoting the association of 3D building blocks, as shown in Fig 14C.

Fig. 14.

When the prbtz is coordinated to a sodium atom presents a bent configuration, with a torsion angle of C1-S2-C8-C9 (77.31°). On the other hand, in the [Co(H₂O)₂(CH₃OH)₄] \cdot 2(prbtz) and [Ni(H₂O)₂(CH₃OH)₄] \cdot 2(prbtz) compounds, where prbtz is outside from the metal coordination sphere is stabilized an extended conformation, with torsion angles of 173.01° and 173.29° respectively, for the same atoms, Fig 15.

Fig. 15.

The full structure of these octahedral coordination compounds is generated by symmetry. The coordination sphere of the metal atom is constituted by six oxygen atoms from two water molecules and four methanol molecules. The metal complex $[M(H_2O)_2(CH_3OH)_4]^{2+}$ is enclosed by four $prbtz^-$ anions, constituting the second coordination sphere through moderate hydrogen bonding interactions, O4-H4A \cdots O3, 1.941Å; O4-H4B \cdots O2, 1.973Å; O5-H5A \cdots O1, 1.916Å; O6-H6A \cdots O1, 1.921Å. Fig 16

Fig. 16.

Different stacking contacts are observed between three $prbtz^-$ molecules, C8-H8A $\cdots\pi$ (benzene ring) in a face to edge orientation (2.800Å); lp(S1) $\cdots\pi$ (heterocycle ring) (3.583Å) and lp(S2) $\cdots\pi$ (heterocycle ring) (3.459Å). The spacefill representation shows the interaction of the S lone pair, from the aliphatic chain, with the heterocyclic rings, Fig. 17.

Fig. 17.

The supramolecular structure stabilizes an intercalated anion-cation-anion giving place to a 3D arrangement, Fig. SI 10

Theoretical calculations

In order to analyze the stability and the interactions of the benzothiazole compounds, all electron calculations were realized for the bis-benzothiazole (ebbtz). For this study, a model of two layers of ebbtz was selected. The theoretical results allowed the determination of the main binding interactions responsible for the stability for this benzothiazole systems, π -stacking, S lone pair $\cdots\pi$, N \rightarrow S intermolecular interactions.

These interactions take place at the frontier molecular orbitals, as it is shown in Fig. 18. The highest occupied molecular orbital (HOMO, -6.50eV) contains the non-covalent sulfur lone pair $\cdots\pi$

interaction. At lower energy (-6.95eV), appears the π stacking between the six membered ring and the thiazole ring. Moreover, a N \rightarrow S intermolecular interaction is displayed by the lowest occupied molecular orbital (LUMO, -2.25eV). The intermolecular interactions, π -stacking, S lone pair $\cdots\pi$, N \rightarrow S add up to 81.22 kJ/mol, which is the stabilization energy between two layers of ebbtz. Note that a large HOMO-LUMO separation (4.25eV) is consistent with the structural stability of the system. The weak interactions observed in the crystal structure of ebbtz are in agreement with the theoretical results.

Fig. 18.

5. Conclusions

This study of weak interactions in the benzothiazole derivatives and their coordination compounds, contributed to the understanding of the preferred conformations and associations of these molecules on their supramolecular arrangements.

The bis-benzothiazole (ebbtz) and the sulfonate-benzothiazole (prbtz) stabilized an extended conformation, with intra and intermolecular N \rightarrow S interactions, when they were not coordinated. Upon coordination to a metal ion, a bent conformation was preferred.

The supramolecular arrangements of these sulfur-containing compounds are governed by several and cooperative weak interactions, where the behavior of the sulfur atom, as Lewis base or Lewis acid, was relevant. All compounds presented H-bonding, $\pi\cdots\pi$ stacking (eclipsed, head-to-tail or T-shape) and lp(S) $\cdots\pi$ interactions with the aromatic benzothiazole rings.

Theoretical calculations indicated that $\pi\cdots\pi$ stacking and S lone pair $\cdots\pi$ interactions occur at the most external molecular orbitals, LUMO and HOMO. As well as the N \rightarrow S interaction was found at the HOMO-7 orbital.

Acknowledgments

Financial support from Conacyt, grant CB2012-178851 and DGAPA postdoctoral fellowship and grant IN224516, is acknowledged.

Supplementary data

CCDC data contains the supplementary crystallographic data for: 1562798 $[\text{Cu}_2(\mu\text{-Br})_3(\text{ebtz})\text{Br}]_n$; 1562799 btzca; 1562800 ebbtz; 1562801 $[\text{Cu}(\text{MeO-ebtz})\text{Cl}]\text{Cl}\cdot 4\text{H}_2\text{O}$; 1562802 $[\text{Co}(\text{H}_2\text{O})_2(\text{CH}_3\text{OH})_4]\cdot 2(\text{prbtz})$; 1562803 $[\text{Na}_2(\text{prbtz})_2(\text{H}_2\text{O})_2\mu\text{-}(\text{H}_2\text{O})]_n$; 1562804 $[\text{Ni}(\text{H}_2\text{O})_2(\text{CH}_3\text{OH})_4]\cdot 2(\text{prbtz})$ and 1562805 $[\text{Cu}(\text{ebtz})\text{Br}]\text{Br}\cdot \text{H}_2\text{O}$. These data can be obtained free of charge via <http://www.ccdc.cam.ac.uk/conts/retrieving.html>, or from the Cambridge Crystallographic Data Centre, 12 Union Road, Cambridge CB2 1EZ, UK; fax: (+44) 1223-336-033; or e-mail: deposit@ccdc.cam.ac.uk.

Supplementary Information

^1H and ^{13}C NMR spectra of ebbtz and btzca compounds and 3D supramolecular arrangements of all the obtained compounds are given in Fig. SI 1 to Fig. SI 10.

6. References

- [1] T. Steiner, *Angew. Chem. Int. Ed.* 41 (2002) 48–76.
- [2] G.N. Pairas, P.G. Tsoungas, *ChemistrySelect.* 1 (2016) 4520–4532.
- [3] J.-A. van den Berg, K.R. Seddon, *Cryst. Growth Desing.* 3 (2003) 643–661.
- [4] E.A. Meyer, R.K. Castellano, D. Franois, *Angew. Chem. Int. Ed.* 42 (2003) 1210–1250.
- [5] J.W. Steed, *Supramolecular chemistry*, LONDON, UK, 2005.
- [6] R.E. Rosenfield, R. Parthasarathy, J.D. Dunitz, *J. Am. Chem. Soc.* 99 (1977) 4860–4862.
- [7] T.N. Guru Row, R. Parthasarathy, *J. Am. Chem. Soc.* 103 (1981) 477–479.
- [8] M. Iwaoka, S. Takemoto, M. Okada, S. Tomoda, *Bull. Chem. Soc. Jpn.* 75 (2002) 1611–1625.
- [9] A.A. Milov, R.M. Minyaev, V.I. Minkin, *J. Phys. Chem. A* 2011,. 115 (2011) 12973–12982.
- [10] V.D.P.N. Nziko, S. Scheiner, *J. Phys. Chem. A* 2014,. 118 (2014) 10849–10856.
- [11] M. Iwaoka, S. Takemoto, S. Tomoda, *J. Am. Chem. Soc.* 124 (2002) 10613–10620.
- [12] R. Colorado-Peralta, C. Guadarrama-Pérez, L.A. Martínez-Chavando, J.C. Gálvez-Ruiz,

- A.M. Duarte-Hernández, G. V. Suárez-Moreno, A. Vásquez-Badillo, S.A. Sánchez-Ruiz, R. Contreras, A. Flores-Parra, *J. Organomet. Chem.* 751 (2014) 579–590.
- [13] Z. García-Hernández, A. Flores-Parra, J.M. Grevy, Á. Ramos-Organillo, R. Contreras, *Polyhedron*. 25 (2006) 1662–1672.
- [14] M. Iwaoka, N. Isozumi, *Molecules*. 17 (2012) 7266–7283.
- [15] M. Iwaoka, N. Isozumi, *Biophysics*, 2 (2006) 23–34.
- [16] A. Peña-Hueso, F. Téllez, R. Vieto-Peña, R.O. Esquivel, A. Esparza-Ruiz, I. Ramos-García, R. Contreras, N. Barba-Behrens, A. Flores-Parra, *J. Mol. Struct.* 984 (2010) 409–415.
- [17] E.W. Reinheimer, M. Fourmigué, K.R. Dunbar, *J. Chem. Crystallogr.* 39 (2009) 723–729.
- [18] S. Biswas, G.P.A. Yap, K. Dey, *Polyhedron*. 28 (2009) 3094–3100.
- [19] A. Esparza-Ruiz, A. Peña-Hueso, J. Hernández-Díaz, A. Flores-Parra, R. Contreras, *Cryst. Growth Des.* 7 (2007) 2031–2040.
- [20] T.J. Mooibroek, P. Gamez, J. Reedijk, *CrystEngComm*. 10 (2008) 1501.
- [21] M. Egli, S. Sarkhel, *Acc. Chem. Res.* 40 (2007) 197–205.
- [22] J. Novotný, S. Bazzi, R. Marek, J. Kozelka, *Phys. Chem. Chem. Phys.* 18 (2016) 19472–19481.
- [23] Y. Nagao, H. Iimori, S. Goto, T. Hirata, S. Sano, H. Chuman, M. Shiro, *Tetrahedron Lett.* 43 (2002) 1709–1712.
- [24] M.K. Si, R. Lo, B. Ganguly, *Chem. Phys. Lett.* 631–632 (2015) 6–11.
- [25] M.R. Koebel, A. Cooper, G. Schmadeke, S. Jeon, M. Narayan, S. Sirimulla, *J. Chem. Inf. Model.* 2016, 56 (2016) 2298–2309.
- [26] Y. Nagao, T. Honjo, H. Iimori, S. Goto, S. Sano, M. Shiro, K. Yamaguchi, Y. Sei, *Tetrahedron Lett.* 45 (2004) 8757–8761.
- [27] T. Honda, H. Tajima, Y. Kaneko, M. Ban, T. Inaba, Y. Takeno, K. Okamoto, H. Aono, *Bioorganic Med. Chem. Lett.* 18 (2008) 2939–2943.
- [28] Y. Nagao, T. Hirata, S. Goto, S. Sano, A. Kakehi, K. Iizuka, M. Shiro, *J. Am. Chem. Soc.* 120 (1998) 3104–3110.
- [29] S. Lin, S.T. Wroblewski, J. Hynes, S. Pitt, R. Zhang, Y. Fan, A.M. Doweyko, K.F. Kish, J.S. Sack, M.F. Malley, S.E. Kiefer, J.A. Newitt, M. McKinnon, J. Trzaskos, J.C. Barrish, J.H. Dodd, G.L. Schieven, K. Leftheris, *Bioorganic Med. Chem. Lett.* 20 (2010) 5864–5868.
- [30] K. Hayashi, S. Ogawa, S. Sano, M. Shiro, K. Yamaguchi, Y. Sei, Y. Nagao, *Chem. Pharm.*

- Bull. (Tokyo). 56 (2008) 802–6.
- [31] M. Feng, B. Tang, S.H. Liang, X. Jiang, *Curr. Top. Med. Chem.* 16 (2016) 1200–1216.
- [32] L.M. Espinoza-Fonseca, J.G. Trujillo-Ferrara, *Biochem. Biophys. Res. Commun.* 328 (2005) 922–928.
- [33] R. Chávez-Calvillo, M. Costas, J. Hernández-Trujillo, *Phys. Chem. Chem. Phys.* 12 (2010) 2067–2074.
- [34] N. Hassan, M.P. Gárate, T. Sandoval, L. Espinoza, Á. Piñeiro, J.M. Ruso, *Langmuir*. 26 (2010) 16681–16689.
- [35] G.M. Sheldrick, *Acta Crystallogr. Sect. A Found. Crystallogr.* 64 (2007) 112–122.
- [36] B. Jianming, R. Beresis, R. Berger, S. L. Colletti, S. Miao, W. Parson, K. M. Rupprecht, J. N. Johanson, F. Kayser, E. W. Kovacs. WO Patent 2004058763 (A1), July 15, (2004).
- [37] A.D. Becke, *J. Chem. Phys.* 98 (1993) 5648–5652.
- [38] C. Lee, W. Yang, R.G. Parr, *Phys. Rev. B.* 37 (1988) 785–789.
- [39] A.D. McLean, G.S. Chandler, *J. Chem. Phys.* 72 (1980) 5639–5648.
- [40] A.J.H. Wachters, *J. Chem. Phys.* 52 (1970) 1033–1036.
- [41] T. Clark, J. Chandrasekhar, G.W. Spitznagel, P.V.R. Schleyer, *J. Comput. Chem.* 4 (1983) 294–301.
- [42] Gaussian 09, Revision D.01, M. J. Frisch, G. W. Trucks, H. B. Schlegel, G. E. Scuseria, M. A. Robb, J. R. Cheeseman, G. Scalmani, V. Barone, B. Mennucci, G. A. Petersson, H. Nakatsuji, M. Caricato, X. Li, H. P. Hratchian, A. F. Izmaylov, J. Bloino, G. Zheng, J. L. Sonnenberg, M. Hada, M. Ehara, K. Toyota, R. Fukuda, J. Hasegawa, M. Ishida, T. Nakajima, Y. Honda, O. Kitao, H. Nakai, T. Vreven, J. A. Montgomery, Jr., J. E. Peralta, F. Ogliaro, M. Bearpark, J. J. Heyd, E. Brothers, K. N. Kudin, V. N. Staroverov, T. Keith, R. Kobayashi, J. Normand, K. Raghavachari, A. Rendell, J. C. Burant, S. S. Iyengar, J. Tomasi, M. Cossi, N. Rega, J. M. Millam, M. Klene, J. E. Knox, J. B. Cross, V. Bakken, C. Adamo, J. Jaramillo, R. Gomperts, R. E. Stratmann, O. Yazyev, A. J. Austin, R. Cammi, C. Pomelli, J. W. Ochterski, R. L. Martin, K. Morokuma, V. G. Zakrzewski, G. A. Voth, P. Salvador, J. J. Dannenberg, S. Dapprich, A. D. Daniels, O. Farkas, J. B. Foresman, J. V. Ortiz, J. Cioslowski, and D. J. Fox, Gaussian, Inc., Wallingford CT, 2013.

Table 1.

Crystal data and structure refinement for benzothiazole derivatives and their coordination compounds

Data	btzca	ebbtz	[Cu(MeO-ebbtz)Cl]Cl·4H ₂ O	[Cu ₂ (μ-Br) ₃ (ebtz)Br] _n	[Cu(ebtz)Br]Br·H ₂ O
Chemical formula	C ₈ H ₅ NOS	C ₁₈ H ₁₄ N ₄ S ₂	C ₂₀ H ₃₀ N ₄ O ₆ S ₂ Cl ₂ Cu	C ₁₀ H ₁₁ Br ₄ Cu ₂ N ₃ S	C ₂₀ H ₂₈ Br ₄ Cu ₂ N ₆ O ₃ S ₂
F. W (g mol ⁻¹)	163.19	350.45	621.04	651.98	911.31
T (K)	293(2)	293(2)	293(2)	293(2)	150(2)
Crystal system	Orthorhombic	Monoclinic	Triclinic	Monoclinic	Monoclinic
Space group	Pnma	P2 ₁ /c	P $\bar{1}$	P2 ₁ /c	P2 ₁ /c
a (Å)	13.484(3)	16.361(3)	7.7787(16)	7.2963(15)	7.6036(7)
b (Å)	6.5285(13)	4.6924(9)	13.178(3)	7.5256(15)	7.7508(9)
c (Å)	8.5603(17)	22.304(5)	13.669(3)	31.550(6)	26.014(3)
α (°)	90	90	100.00(3)	90	90
β (°)	90	106.16(3)	93.28(3)	91.58(3)	97.865(3)
γ (°)	90	90	93.45(3)	90	90
V (Å ³)	753.6(3)	1644.7(6)	1374.1(5)	1731.72(6)	1518.7(3)
Z	4	4	2	4	2
D _{calc} (mg/m ³)	1.438	1.415	1.501	2.501	1.993
Absorption Coefficient (mm ⁻¹)	0.361	0.330	1.182	11.797	6.833
F(000)	336	728	642	1224	888
Crystal size (mm)	0.5422 x 0.5169 x 0.4118	0.4807 x 0.1176 x 0.0215	0.3282 x 0.0894 x 0.0462	0.150x0.051x0.034	0.129x 0.108x 0.037
Data collected/unique	31585 / 1012	6996 / 3352	10348 / 5611	3164 / 1910	47714 / 27495
Restraints/parameters	0 / 67	0 / 217	60 / 378	82/195	0/179
Goodness of fit (S)	1.125	1.047	1.020	1.042	1.029
R1, wR2[I>2σ(I)]	0.0318, 0.0924	0.0476, 0.1069	0.0484, 0.0993	0.0650, 0.0978	0.0936, 0.2256
R1, wR2(all data)	0.0361, 0.0967	0.0768, 0.1228	0.0866, 0.1185	0.1224, 0.1147	0.1622, 0.2699
Largest difference peak and hole (e. Å ⁻³)	0.246 and -0.193	0.257 and -0.318	0.438 and -0.285	0.798 and -0.679	5.225 and -4.704

$$R_{\text{int}} = \frac{\sum |F_o^2 - \langle F_o^2 \rangle|}{\sum F_o^2}, R_1 = \frac{\sum \|F_o\| - |F_c|}{\sum |F_o|}, wR_2 = \left[\frac{\sum w(F_o^2 - F_c^2)^2}{\sum w(F_o^2)^2} \right]^{1/2}$$

Table 2

Crystal data and structure refinement for benzothiazole derivatives and their coordination compounds

Data	[Na ₂ (prbtz) ₂ (H ₂ O) ₂ μ-H ₂ O] _n	[Ni(H ₂ O) ₂ (CH ₃ OH) ₄]-2(prbtz)	[Co(H ₂ O) ₂ (CH ₃ OH) ₄]-2(prbtz)
Chemical formula	C ₂₀ H ₂₆ N ₂ Na ₂ O ₉ S ₆	C _{23.47} H ₄₀ N ₂ Ni O _{12.53} S ₆	C _{23.87} H ₄₀ Co N ₂ O _{12.13} S ₆
F. W (g mol ⁻¹)	676.77	801.76	800.39
T (K)	130 (2)	130 (2)	130(2)
Crystal system	Monoclinic	Triclinic	Triclinic
Space group	C2/c	P $\bar{1}$	P $\bar{1}$
a (Å)	43.516(9)	6.8892(14)	6.8627(14)
b (Å)	5.5768(11)	7.5577(15)	7.5786(15)
c (Å)	11.301(2)	16.709(3)	16.857(3)
α (°)	90.0	93.71(3)	94.30(3)
β (°)	90.96(3)	93.13(3)	93.08(3)
γ (°)	90.0	100.14(3)	100.11(3)
V (Å ³)	2742.2(10)	852.7(3)	858.7(3)
Z	4	1	1
D _{calc} (mg/cm ³)	1.639	1.562	1.548
Absorption Coefficient (mm ⁻¹)	0.584	0.997	0.924
F(000)	1400	419	417
Crystal size (mm)	0.6027 x 0.4200 x 0.0462	0.4004 x 0.1877 x 0.1784	0.2809 x 0.1492 x 0.1204
Data collected/unique	10670/2683	5820/3358	6426/3384
Restraints/parameters	5 / 186	132 / 271	21/ 238
Goodness of fit (S)	1.092	1.027	1.051
R1, wR2[I>2σ(I)]	R1 = 0.0356, wR2 = 0.0868	R1 = 0.0340, wR2 = 0.0727	R1 = 0.0281, wR2 = 0.0614
R1, wR2(all data)	R1 = 0.0397, wR2 = 0.0894	R1 = 0.0442, wR2 = 0.0786	R1 = 0.0373, wR2 = 0.0649
Largest difference peak and hole (e. Å ⁻³)	0.567 and -0.378	0.330 and -0.360	0.270 and -0.294

$$R_{\text{int}} = \frac{\sum |F_o^2 - \langle F_o^2 \rangle|}{\sum F_o^2}, R_1 = \frac{\sum \|F_o\| - |F_c|}{\sum |F_o|}, wR_2 = \left[\frac{\sum w(F_o^2 - F_c^2)^2}{\sum w(F_o^2)^2} \right]^{1/2}$$

Figure Captions

Fig. 1. ORTEP representation of btzca, with thermal ellipsoids at 30% of probability (left) and hydrogen bonds and preferred conformation O→S are showed (right).

Fig. 2. Structure stabilized by π -stating interactions in btzca.

Fig 3. ORTEP representation of ebbtz with thermal ellipsoids at 30% of probability and angle between the planes of benzothiazole moieties.

Fig 4. Zig-zag arrangement through N→S inter and intramolecular interactions.

Fig 5. Interactions found in the ebbtz crystal A) π stacking, B) T-shape.

Fig 6. ORTEP representation of [Cu(MeO-ebbtz)Cl]Cl·4H₂O compound with thermal ellipsoids at 30% of probability.

Fig 7. Association of H₂O molecules by hydrogen bonding.

Fig 8. Supramolecular structure of [Cu(MeO-ebbtz)Cl]Cl·4H₂O, stabilized by lp(S)⋯ π interactions.

Fig. 9. ORTEP representation (30% thermal ellipsoid probability) of octahedral and tetrahedral geometries for copper(II) atoms in the [Cu₂(μ -Br)₃(ebtz)Br]_n compound.

Fig. 10. Interactions in [Cu₂(μ -Br)₃(ebtz)Br]_n polymer. A) π -stating and lp(S)⋯ π interactions. B) Hydrogen bonding that interconnect the building blocks.

Fig. 11. ORTEP representation for the [Cu(ebtz)Br]Br·H₂O compound, 30% probability.

Fig. 12. Weak interactions, π -stating and lp(S)⋯ π , in [Cu(enbt)Br]Br·H₂O

Fig. 13 Dimeric unit of $[\text{Na}_2(\text{prbtz})_2(\text{H}_2\text{O})_2\mu\text{-(H}_2\text{O)}]_n$, showing the bridging H_2O molecule in the eight membered ring (thermal ellipsoid 30% probability).

Fig. 14 Weak interactions on the c axis of $[\text{Na}_2(\text{prbtz})_2(\text{H}_2\text{O})_2\mu\text{-H}_2\text{O}]_n$ A) $\text{N}\rightarrow\text{S}$ interactions; B) face to edge contacts; C) 3D building blocks association

Fig. 15. In the $[\text{Na}_2(\text{prbtz})_2(\text{H}_2\text{O})_2\mu\text{-(H}_2\text{O)}]_n$, compound, prbtz is coordinated to a sodium atom with a bent conformation (A), while for $[\text{M}(\text{H}_2\text{O})_2(\text{CH}_3\text{OH})_4]\cdot 2(\text{prbtz})$ ($\text{M} = \text{Co}^{\text{II}}, \text{Ni}^{\text{II}}$) compounds, prbtz is not coordinated, adopting a planar conformation (B).

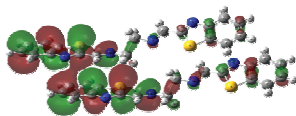
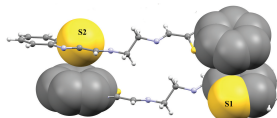
Fig. 16. Second coordination sphere of $[\text{M}(\text{H}_2\text{O})_2(\text{CH}_3\text{OH})_4]^{2+}$ ($\text{M} = \text{Co}^{\text{II}}, \text{Ni}^{\text{II}}$)

Fig. 17. Stacking contacts between neighboring prbtz⁻ molecules, S1 and S2 $\text{lp}\cdots\pi(\text{ring})$

Fig.18. Frontier molecular orbitals for a two layer model of the ebbtz compound.

ACCEPTED MANUSCRIPT

The role of weak interactions in self-assembly of supramolecular associations of benzothiazole derivatives and their coordination compounds

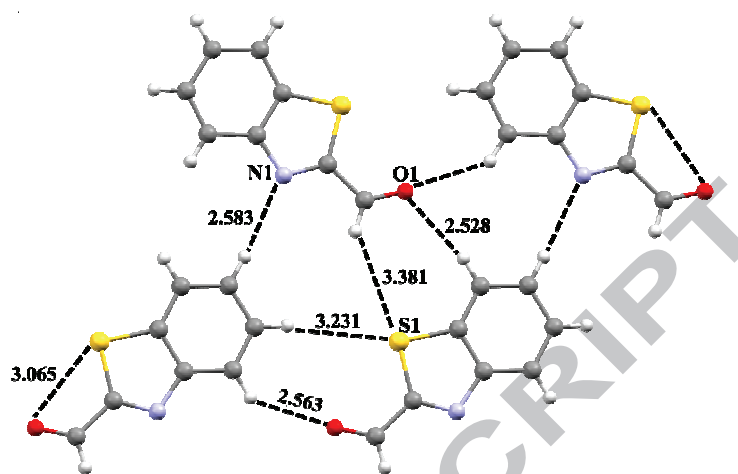
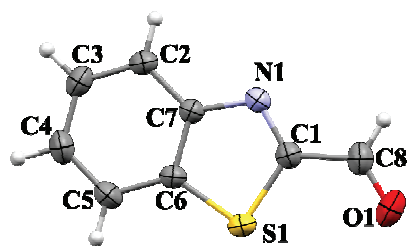


Bis-benzothiazole derivatives and their coordination compounds were synthesized and their weak interactions analyzed. S lone pair $\cdots\pi$, $\pi\cdots\pi$ staking, N \rightarrow S, O \rightarrow S, H $\cdots\pi$ and hydrogen bonding stabilized different supramolecular arrangements. Theoretical calculations showed that the S lone pair $\cdots\pi$ and $\pi\cdots\pi$ interactions take place at the frontier LUMO and HOMO molecular orbitals.

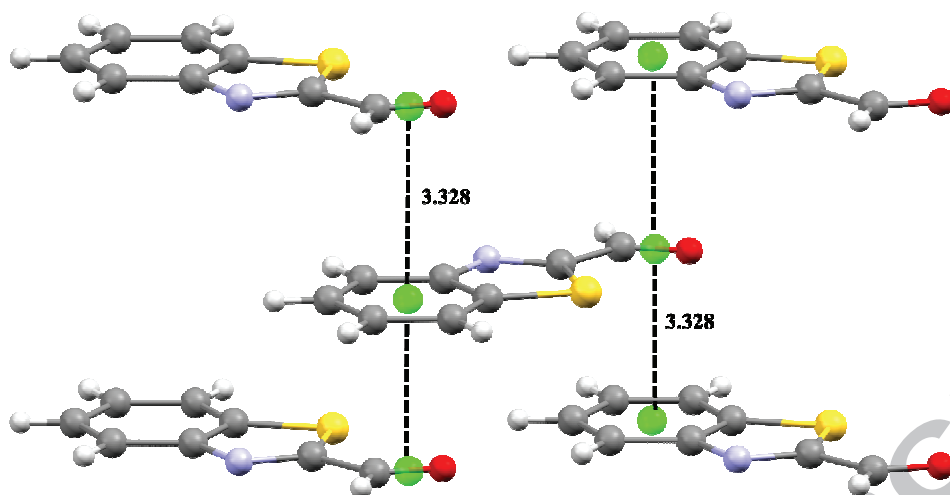
Alma Lilia García-Ortiz, Ricardo Domínguez-González, Margarita Romero-Ávila, Blas Flores-Pérez, Luis Guillén, Miguel Castro, Norah Barba-Behrens*

- 1- Benzothiazole derivatives and coordination compounds
- 2- Synthesis of benzothiazole Schiff bases
- 3- Supramolecular arrangements
- 4- Weak interactions: sulfur (lp) $\cdots\pi$, $\pi\cdots\pi$ stacking, N \rightarrow S, O \rightarrow S and hydrogen bonding.
- 5- Theoretical calculations

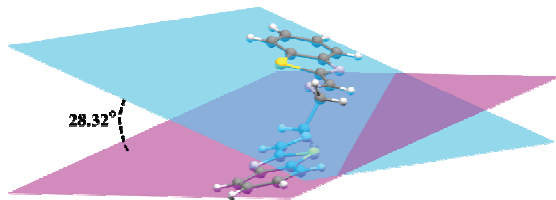
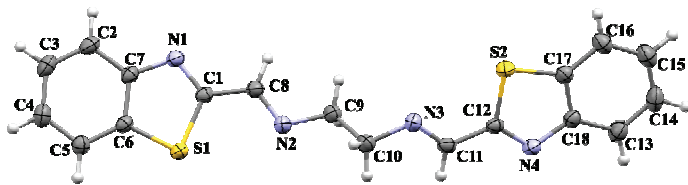
ACCEPTED MANUSCRIPT



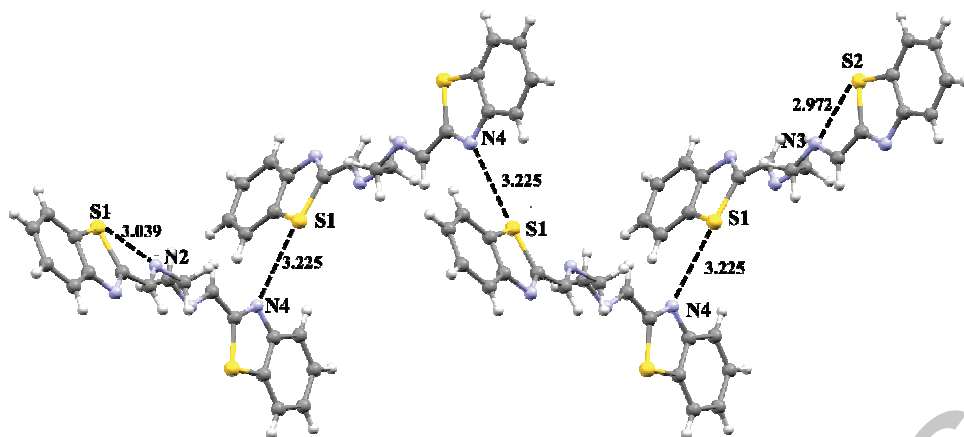
ACCEPTED MANUSCRIPT



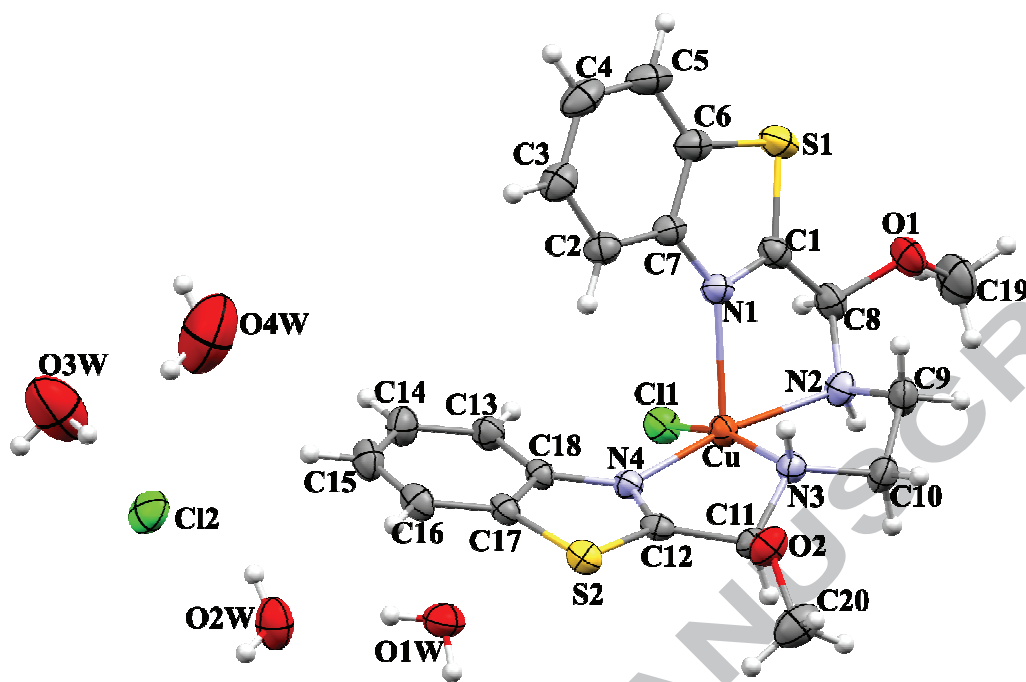
ACCEPTED MANUSCRIPT

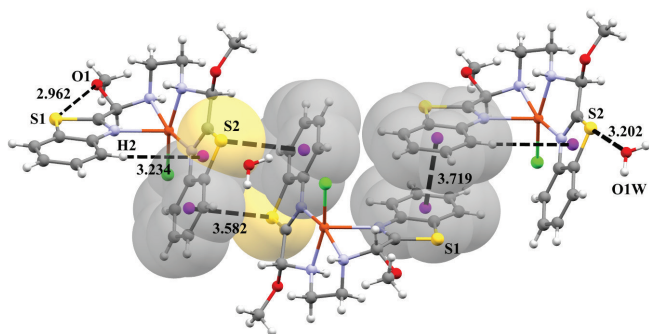


ACCEPTED MANUSCRIPT

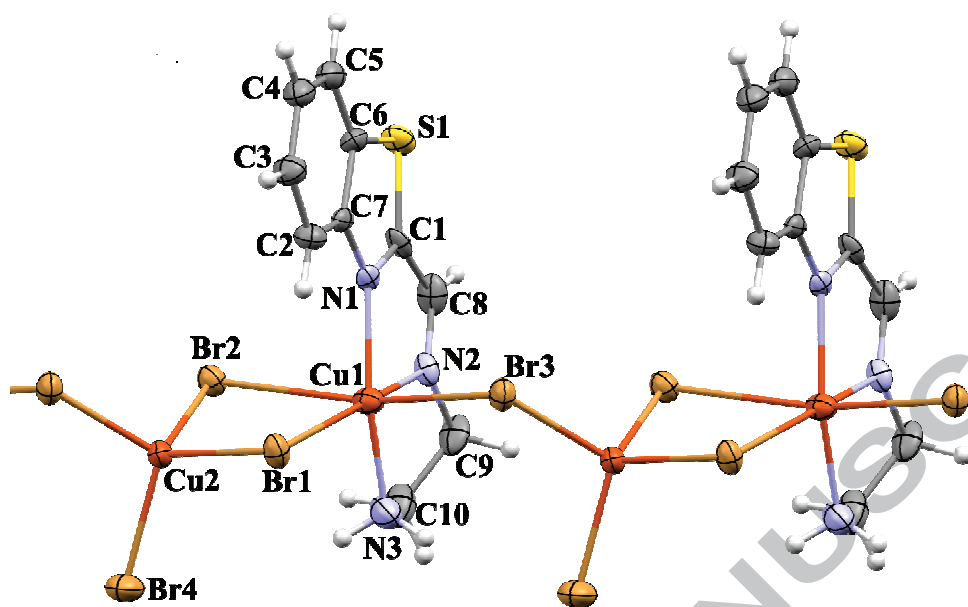


ACCEPTED MANUSCRIPT

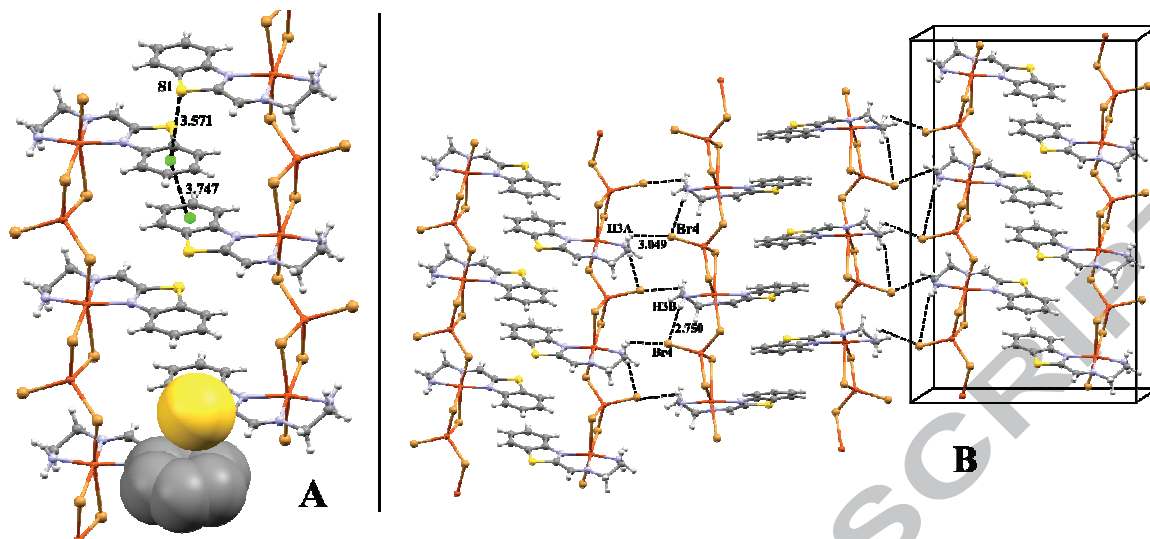




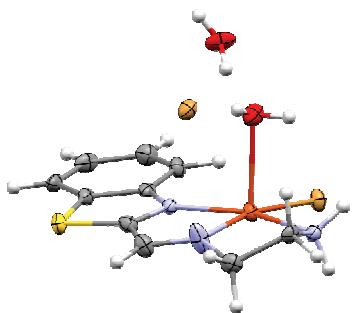
ACCEPTED MANUSCRIPT



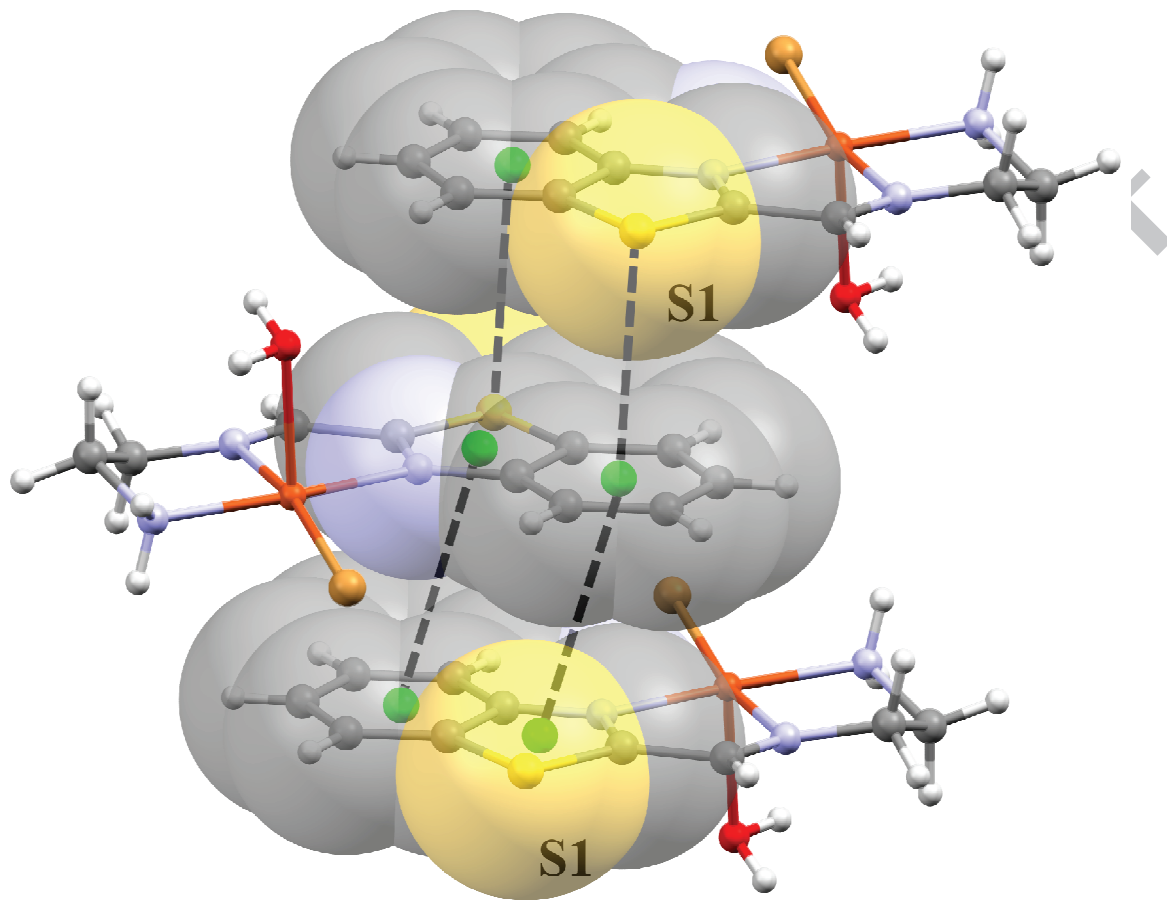
ACCEPTED MANUSCRIPT



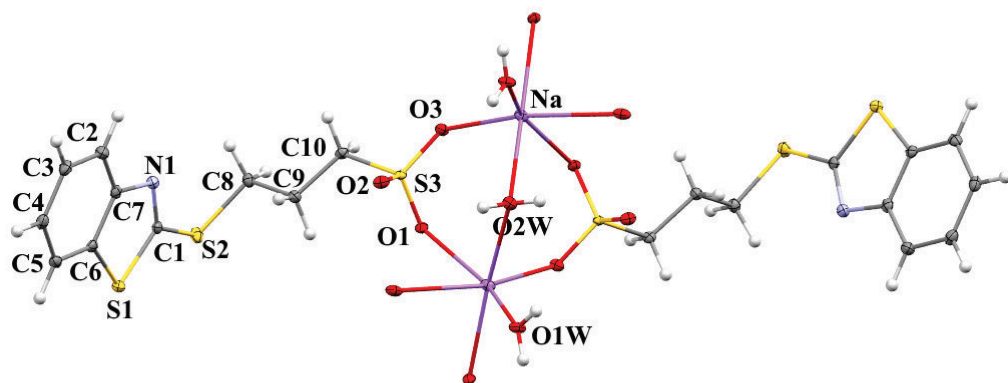
ACCEPTED MANUSCRIPT



ACCEPTED MANUSCRIPT

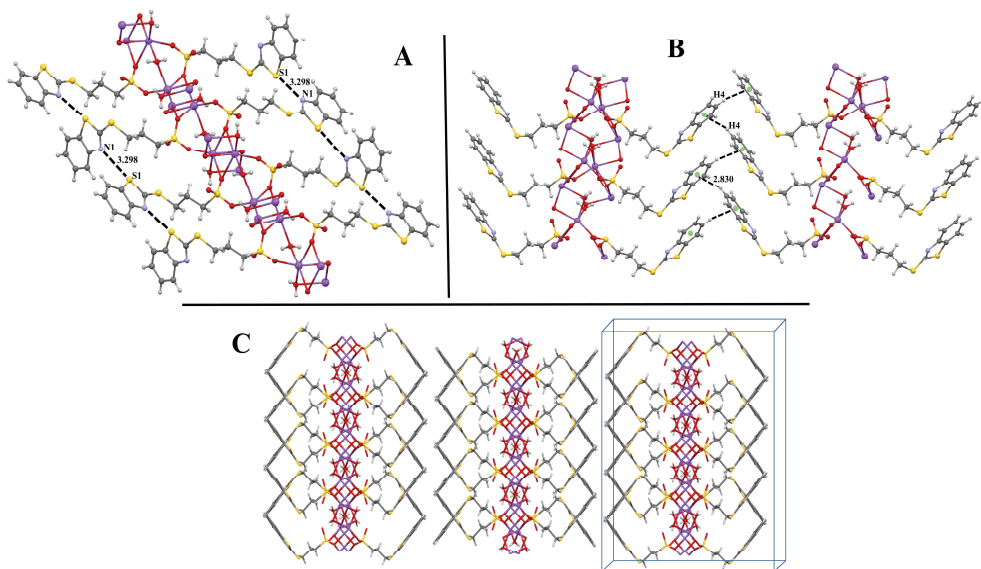


ACCEPTED



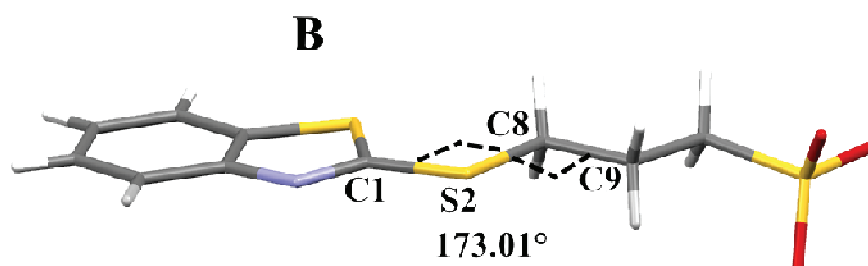
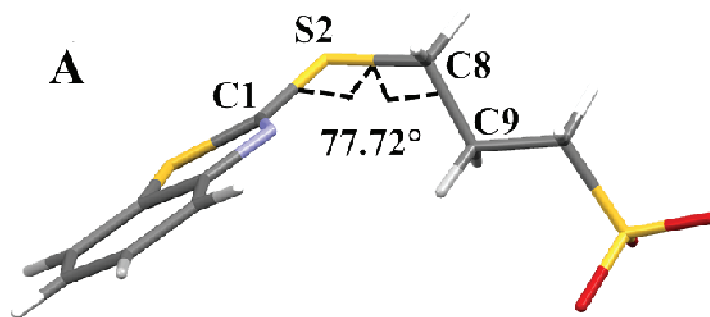
ACCEPTED M.

RIPT



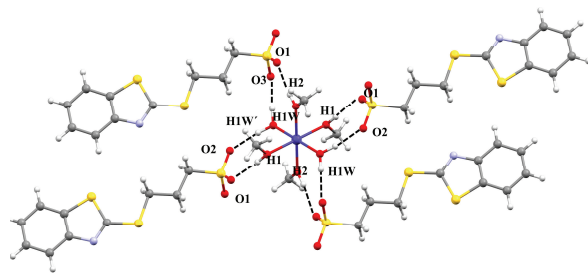
ACCEPTED MANUSCRIPT

RIPT

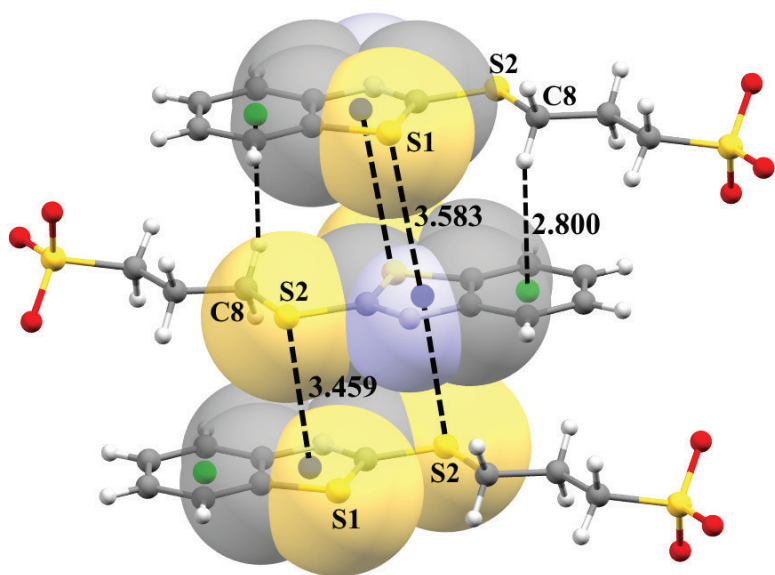


ACCEPTED MANUSCRIPT

RIPT



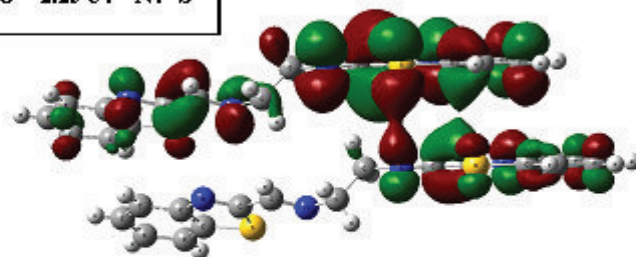
ACCEPTED MANUSCRIPT



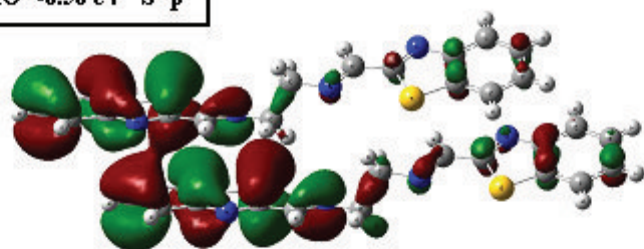
ACCEPTED MANUSCRIPT

SCRIPT

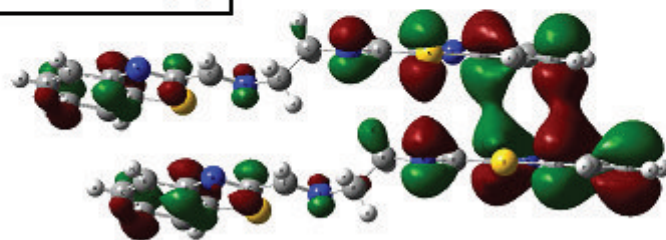
LUMO -2.25 eV N π S



HOMO -6.50 eV S π -p



HOMO-7 -6.95 eV p π -p



ACCEPTED

SCRIPT